Acta Crystallographica Section B
**Structural Science**
ISSN 0108-7681

# The whole range of hydrogen bonds in one crystal structure: neutron diffraction and charge-density studies of *N*,*N*-dimethylbiguanidinium bis(hydrogensquarate)

**Mihaela-Diana Şerb,[a] Ruimin Wang,[b] Martin Meven[c] and Ulli Englert[b]***

[a]Department of Inorganic Chemistry, University POLITEHNICA of Bucharest, Polizu 1, Bucharest 011061, Romania, [b]Institute of Inorganic Chemistry, RWTH Aachen University, Landoltweg. 1, Aachen 52074, Germany, and [c]Forschungsneutronenquelle Heinz Maier-Leibnitz (FRM-II), TU München, Lichtenbergstrasse 1, Garching D-85747, Germany

Correspondence e-mail: ullrich.englert@ac.rwth-aachen.de

Received 26 August 2011
Accepted 18 October 2011

*N*,*N*-Dimethylbiguanidinium bis(hydrogensquarate) features an impressive range of hydrogen bonds within the same crystal structure: neighbouring anions aggregate to a dianionic pair through two strong O—H···O interactions; one of these can be classified among the shortest hydrogen bonds ever studied. Cations and anions in this organic salt further interact *via* conventional N—H···O and nonclassical C—H···O contacts to an extended structure. As all these interactions occur in the same sample, the title compound is particularly suitable to monitor even subtle trends in hydrogen bonds. Neutron and high-resolution X-ray diffraction experiments have enabled us to determine the electron density precisely and to address its properties with an emphasis on the nature of the *X*—H···O interactions. Sensitive criteria such as the Laplacian of the electron density and energy densities in the bond-critical points reveal the incipient covalent character of the shortest O—H···O bond. These findings are in agreement with the precise geometry from neutron diffraction: the shortest hydrogen bond is also significantly more symmetric than the longer interactions.

## 1. Introduction

Hydrogen bonding represents an interaction of paramount importance. In structural biology hydrogen bonds stabilize complex architectures such as the DNA double helix or secondary structures in proteins (Nowick, 2008). Proton transfer along hydrogen bonds can be considered an important reaction step for a variety of chemical systems (Limbach & Manz, 1998). In view of the small mass of the proton and the short displacement in nuclear positions, this transfer has been associated with at least a certain contribution of quantum tunneling along the hydrogen bonds, both for relatively small molecules such as benzoic acids dimers (Neumann *et al.*, 1998) but also for flavoprotein and quinoprotein enzymes (Sutcliffe & Scrutton, 2002). Hydrogen bonds of very different flavours have been used as interactions in crystal engineering and are widely exploited to generate supramolecular systems by design (Roesky & Andruh, 2003; Prins *et al.*, 2001; Braga *et al.*, 2003). Squaric acid can act both as a donor as well as an acceptor for hydrogen bonding (Karle *et al.*, 1996). Strong bases such as biguanide derivatives (Kaljurand *et al.*, 2000) represent interesting partners for squaric acid: They incorporate a characteristic pattern of multiple sites that can donate or accept hydrogen bonds, thereby directing molecular recognition and association (LeBel *et al.*, 2005). Not only the structural consequences, but also the very nature of hydrogen bonds has stimulated discussion: shorter and presumably stronger interactions have been associated with a more

covalent character, longer with predominantly electrostatic character (Gilli *et al.*, 1994, 2004), but the experimental basis is rather limited mostly because well characterized systems with very short donor···acceptor distances are still rare. On the one hand, neutron diffraction may be used for the precise location of the proton in short hydrogen bonds; on the other hand, charge-density studies, followed by topological analysis of the electron density according to the Atoms in Molecules approach (Bader, 1990) have been used to characterize bonds as more or less covalent. The combination of both techniques has been applied to only a few cases of very short *intermolecular* hydrogen bonds, ensuring that the optimum experimental information is exploited. We explicitly mention two examples here:

(i) A well studied system is concerned with the adduct between urea and phosphoric acid (Kostansek & Busing, 1972; Wilson, 2001; Rodrigues *et al.*, 2001) in which the H atom in the short interaction is located almost at the midpoint between donor and acceptor; its precise position has been shown to be a function of temperature (Wilson, 2001).

(ii) In methylammonium hydrogensuccinate (Flensburg *et al.*, 1995), the H atom involved in the short hydrogen bond occupies a special position and the O—H···O interaction is fully symmetric.

At least one case of a short *intra*- rather than an *inter*-molecular hydrogen bond shall also be given: recently, experimental data concerning the H atom in an enolized 1,3-dione has been published; the very short hydrogen bond is asymmetric (Piccoli *et al.*, 2008). A compilation of neutron diffraction experiments on hydrogen bonds with donor···acceptor distances less than 2.6 Å is available in the supporting information[1] for this article.

In this contribution we report the result of a detailed diffraction study of *N*,*N*-dimethylbiguanidinium-bis(hydrogensquarate) (1). In the title compound hydrogen bonds of very different length and presumably strength occur next to each other in the same crystal structure – a very favourable situation to establish subtle trends in electron density. We will provide experimental support for the statement that very short hydrogen bonds can at least in part be regarded as covalent.

## 2. Experimental

### 2.1. Chemicals and reagents

Squaric acid, *N*,*N*-dimethylbiguanide hydrochloride were purchased and used without further purification. The melting point has been determined on a Gallenkamp apparatus and it is non-corrected; pH measurement was determined using a glass electrode.

[1] Supplementary data for this paper are available from the IUCr electronic archives (Reference: SO5054). Services for accessing these data are described at the back of the journal.

### 2.2. Preparation (Şerb, 2009) of *N*,*N*-dimethylbiguanidinium bis(hydrogensquarate), $(C_4H_{13}N_5)(C_4HO_4)_2$ (1)

*N*,*N*-Dimethylbiguanide hydrochloride (497 mg, 3 mmol) and squaric acid (342 mg, 3 mmol) were dissolved in water (40 ml) and then stirred for 1 h at 333 K. The resulting solution was filtered and the pH of the solution was measured (pH = 1.85). Colourless crystals deposited after several days by evaporation at room temperature. Yield: 0.510 g (95.16%); m.p. 478 K; elemental analysis: calc: (%) C 40.34, H 4.23, N 19.6; found: C 40.78, H 3.94, N 19.85.

### 2.3. Diffraction experiments on (1)

X-ray intensity data were collected at 100 K with Mo $K\alpha$ radiation ($\lambda$ = 0.71073 Å) on a Bruker D8 goniometer equipped with an APEX CCD detector. An Oxford Cryosystems 700 controller was used to ensure constant temperature during data collection. Previous work on phase transitions conducted in parallel on single crystals and on powder at 120 K (Hu & Englert, 2005), at 207 K (Hu *et al.*, 2003) and over the temperature range 175–325 K (Lamberts *et al.*, 2011) indicated a reproducibility of better than 2 K and a temperature match of better than 5 K with alternative cooling devices. Frames were collected in $\omega$-scan mode in nine runs with different settings for detector angle $\theta$ and crystal rotation $\varphi$ and integrated with the help of the program *SAINT* (Bruker, 2003).

Neutron diffraction was performed at Forschungs-Neutronenquelle Heinz Maier-Leibnitz (FRM II) on the single-crystal diffractometer (SCD) HEiDi ($\lambda$ = 0.868 Å) at 100 K. HEiDi is a four-circle diffractometer with a closed Eulerian cradle and a single detector optimized for short wavelengths. An Er-foil (0.5 mm thickness) was used to suppress $\lambda/2$ contamination. Temperature stability during the experiment was better than 0.1 K (closed-cycle cryostat Sumitomo SDK110, temperature range 2.2 $< T <$ room temperature). A calibrated cernox sensor at the very end of the cooling finger near the sample position is used to determine the sample temperature. The sample itself is connected to the finger with an aluminium pin and wrapped into aluminium foil to optimize thermal conduction to the cryostat. A vacuum cap and a heat shield keep away the introduction of heat from outside. From many temperature-dependent measurements of phase transitions down to about 2 K we can exclude a thermal gradient larger than 0.5 K between the sensor and the sample in this temperature region. The Bragg data were collected in rocking–scan mode. The program used for data reduction was *PRON*2010.

Crystal data and data collection parameters for both diffraction experiments and convergence results have been compiled in Table 1. Diagrams related to the data quality and completeness are available in the supporting information.

### 2.4. Refinement

The structure was solved by direct methods (*SHELXS*97; Sheldrick, 2008). Refinement on $F^2$ at the independent atom model (IAM) level was conducted with *SHELXL*97 (Shel-

**Table 1**
Experimental details.

For all structures $Z = 2$. $D_x = 1.595$ Mg m$^{-3}$. Experiments were carried out at 100 K. Refinement was with 0 restraints.

| | Multipole | IAM | Neutron |
|---|---|---|---|
| Crystal data | | | |
| Chemical formula | $C_{12}H_{15}N_5O_8$ | $C_{12}H_{15}N_5O_8$ | $C_{12}H_{15}N_5O_8$ |
| $M_r$ | 357.29 | 357.29 | 357.29 |
| Crystal system, space group | Triclinic, $P\bar{1}$ | Triclinic, $P\bar{1}$ | Triclinic, $P\bar{1}$ |
| $a, b, c$ (Å) | 7.0689 (2), 8.5538 (2), 13.0736 (3) | 7.0689 (2), 8.5538 (2), 13.0736 (3) | 7.0689 (2), 8.5538 (2), 13.0736 (3) |
| $\alpha, \beta, \gamma$ (°) | 90.4260 (9), 105.1180 (9), 102.4250 (10) | 90.4259 (9), 105.1185 (9), 102.4251 (10) | 90.4260 (9), 105.1180 (9), 102.4250 (10) |
| $V$ (Å$^3$) | 743.58 (3) | 743.58 (3) | 743.58 (3) |
| Radiation type | Mo $K\alpha$ | Mo $K\alpha$ | Neutron, $\lambda = 0.86800$ Å |
| $\mu$ (mm$^{-1}$) | 0.14 | 0.14 | 0.15 |
| Crystal size (mm) | 0.38 × 0.21 × 0.13 | 0.38 × 0.21 × 0.13 | 3.0 × 3.5 × 3.5 |
| Data collection | | | |
| Diffractometer | CCD area detector | CCD area detector | Closed Eulerian cradle HEiDi |
| No. of measured, independent and observed [$I > 2\sigma(I)$] reflections | 38 327, 15 808, 9502 | 38 327, 15 808, 9502 | 7815, 5560, 4116 |
| $R_{int}$ | 0.046 | 0.046 | 0.073 |
| $(\sin\theta/\lambda)_{max}$ (Å$^{-1}$) | 1.112 | 1.112 | 0.821 |
| Completeness to $(\sin\theta/\lambda)_{max}$ | 0.924 | 0.924 | 0.808 |
| Refinement | | | |
| Refinement on | $F^2$ | $F^2$ | $F^2$ |
| $R1$ (obs) | 0.034 | 0.050 | 0.061 |
| $R1$ (all) | 0.072 | 0.082 | 0.091 |
| $wR2$ | 0.047 | 0.106 | 0.156 |
| $S$ | 1.05 | 1.07 | 1.14 |
| No. of reflections | 15 808 | 15 808 | 5560 |
| No. of parameters | 950 | 286 | 362 |
| $\Delta\rho_{max}$, $\Delta\rho_{min}$ (e Å$^{-1}$) | 0.13, −0.12 | 0.82, −0.44 | 0.10, −0.17 |

drick, 2008). Anisotropic displacement parameters were assigned to non-H atoms and H atoms were included in idealized geometry. Multipole refinements on $F^2$ based on the Hansen–Coppens formalism for aspheric atomic density expansion (Hansen & Coppens, 1978) were carried out with the program *XD*2006 (Volkov *et al.*, 2006). Multipoles up to hexadecapoles were refined for O, N and C atoms and up to quadrupoles for H atoms involved in classical hydrogen bonds. For the remaining methyl-H atoms, monopoles and bond-oriented dipoles were considered in the multipole refinements. An alternative refinement based on structure factors and multipoles up to octopoles for the non-H atoms gave qualitatively similar results, albeit with higher standard uncertainties and slower convergence due to the smaller number of data.

Although both X-ray and neutron diffraction were conducted at the same nominal temperature, a comparison of $U_{eq}$ for non-H atoms after convergence revealed systematic differences. A similar effect had been described by Flensburg *et al.* (1995). The resulting parameters could be related by the linear expression

$$U_N = 1.054(0.050)U_x + 0.00515(0.00062). \quad (1)$$

In order to ensure the proper treatment of anisotropic displacement parameters for H atoms in the multipole refinement of the high-resolution X-ray data, they were not simply transferred from the neutron experiment but diagonalized according to

$$U_{diag} = V^{-1}U_N V \quad (2)$$

The resulting eigenvalues were scaled with $U_{diag'} = (U_{diag} - 0.00515)/1.054$ and ellipsoids of the original orientation, suitable for X-ray refinement, were re-generated by

$$U_X = VU_{diag'}V^{-1}. \quad (3)$$

In the final multipole refinement, contraction parameters $\kappa$ and $\kappa'$ for non-H atoms were freely refined. $\kappa$ and $\kappa'$ for H were fixed to 1.2 and 1.0, respectively.

For the final structure model based on the combination of X-ray and neutron data, the rigid-bond test (Hirshfeld, 1976) was satisfactory, with a maximum difference in mean-square displacement amplitudes along a covalent bond of 0.0012 (3) Å$^2$ in the cation and of 0.0004 (2) Å$^2$ in one of the anions in the crystal structure of (1).

## 3. Results and discussion

In the solid state the title compound consists of dications and pairs of monoanions as shown in the scheme.

**Table 2**
Geometric and electronic properties of the selected hydrogen bonds represented in Fig. 2.

| Interaction in Fig. 2 | O1—H1···O6 *A* | O5—H5···O2 *B* | N2$^{i}$—H2$^{i}$···O4 *C* | N4$^{ii}$—H4*B*$^{ii}$···O7 *D* | C9$^{ii}$—H9*A*$^{ii}$···O6 *E* |
|---|---|---|---|---|---|
| $D_{D\cdots A}$ (Å) | 2.447 (3) | 2.568 (3) | 2.742 (2) | 3.008 (2) | 3.211 (3) |
| $D_{D-H}$ (Å) | 1.048 (4) | 1.022 (4) | 1.034 (4) | 1.010 (4) | 1.070 (7) |
| $D_{H\cdots A}$ (Å) | 1.421 (4) | 1.569 (4) | 1.779 (4) | 2.068 (5) | 2.265 (7) |
| $\angle D-H\cdots A$ (°) | 164.6 (4) | 164.5 (4) | 153.2 (3) | 154.1 (4) | 146.3 (5) |
| $\rho$ (e Å$^{-3}$)† | 0.64 (2) | 0.37 (2) | 0.24 (2) | 0.090 (9) | 0.072 (4) |
| $\nabla^2\rho$ (e Å$^{-5}$)† | 2.43 (5) | 3.14 (4) | 3.69 (3) | 2.21 (2) | 1.391 (2) |
| $G$ (a.u.)† | 0.073 | 0.044 | 0.038 | 0.017 | 0.011 |
| $V$ (a.u.)† | −0.121 | −0.055 | −0.038 | −0.012 | −0.008 |
| $\lvert V\rvert/G$ | 1.66 | 1.26 | 1.00 | 0.71 | 0.72 |
| $G/\rho$ (a.u.)† | 0.770 | 0.803 | 1.07 | 1.27 | 1.03 |

Symmetry codes: (i) $1+x, 1+y, z$; (ii) $2-x, 1-y, 1-z$. † $\rho$, $\nabla^2\rho$, $G$ and $V$ represent the electron density, its Laplacian, the kinetic and the potential energy density at the bond-critical point.

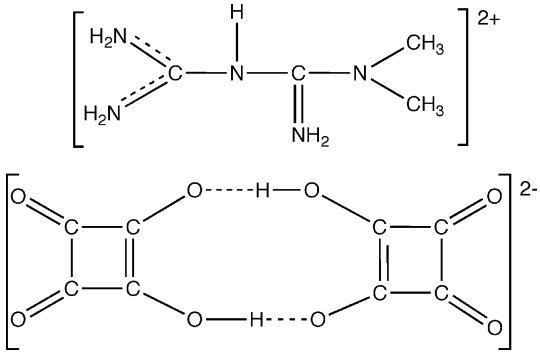


The overall hydrogen-bond pattern in (1) is complex and requires closer inspection. Interatomic distances and angles discussed in this context are based on the significantly more reliable results of the neutron diffraction experiment. Fig. 1 shows a displacement ellipsoid plot of the asymmetric unit of (1) as deduced from the neutron data.

Two hydrogen monosquarate anions interact *via* the shortest hydrogen bonds which exist in the crystal structure. The resulting aggregation is at first sight reminescent of the popular carboxylic acid dimer which was identified as a synthon by Desiraju (1995); the analogy is, however, misleading, because (1) involves two negatively charged moieties rather than two neutral molecules. Such a short contact between two anions seems counterintuitive; it is, however, rather popular between species which are not fully deprotonated where a positively charged H atom connects these residues by a hydrogen bond. In (1) the short O—H···O bonds within the anionic dimer form between a protonated H donor and a deprotonated H acceptor group of the same chemical species, namely hydrogensquarate; hence the contributing moieties ideally match the p$K_a$ equalization principle (Gilli *et al.*, 2009). According to this concept, short O—H···O interactions may be expected between conjugate acid–base pairs. These short hydrogen bonds do not generate a fully symmetric dianionic residue: the donor···acceptor distances in the hydrogen bonds amount to 2.447 (3) and 2.568 (3) Å, and hence differ significantly from the geometric point of view; the electronic differences will be discussed below. The dianion does not constitute an isolated residue but rather a charged acceptor for all potential H donors from the surrounding cations: seven classical N—H···O contacts occur between cations and anions in crystalline (1), subtending a range of donor···acceptor distances between 2.742 (2) Å for the shortest and 3.008 (2) Å for the longest interaction. In addition to these conventional hydrogen bonds, non-classical C—H···O interactions occur between methyl H atoms in the cations and O atoms of the anions; they are characterized by even longer donor···acceptor separations of *ca* 3.2 Å. It is a remarkable feature of crystalline (1) that all the above-mentioned interactions may be associated with hydrogen bonding in a more general sense and that they cover an impressive distance range. Five of these contacts, namely the two O—H···O bonds in the dianionic pair, the shortest and the longest N—H···O bond between cations and anions, and one of the non-classical hydrogen bonds, have been discussed in detail in this article. Important properties of these selected hydrogen bonds have been compiled in Table 2. A comparison of the geometric and electronic features of all the hydrogen bonds is provided in Table S3 of the supporting information.

The presence of distinctly different hydrogen bonds in the same structure offers the rare possibility of monitoring two

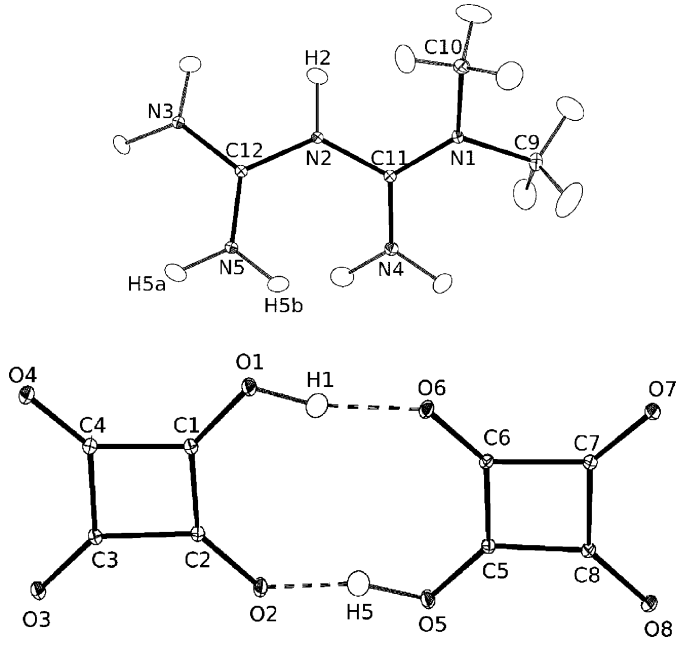


**Figure 1**
Displacement ellipsoid plot of a dication and a dianion in (1); ellipsoids at the 30% probability level (Spek, 2009).

criteria of hydrogen-bond strength without any necessity for external scaling.

(i) Shorter H···*A* interactions are commonly associated with stronger hydrogen bonds; this relationship holds true for a wide range of interatomic distances. The concomitant effect of significantly elongated *D*—H distances with respect to a standard single bond (Steiner, 2002) is only observed for short hydrogen bonds.

(ii) Stronger hydrogen bonds are expected to show higher electron density; in high-resolution X-ray diffraction experiments, this quantity and its derived properties become observable at the bond-critical point along the hydrogen···acceptor bond path.

We will first address the distance criterion. All interatomic distances quoted in Table 2 refer to the results of the low-temperature single-crystal neutron diffraction experiment.

Following the commonly accepted trend that atomic radii decrease in the order C > N > O for covalent bonds (Cordero *et al.*, 2008), terminal oxygen–hydrogen should be shorter than nitrogen–hydrogen bonds. Table 2 shows that the situation is more complex in the title compound in which all H atoms are involved in hydrogen bonds: The two O—H···O interactions differ with respect to their donor···acceptor distances, and the shorter hydrogen bond O1—H1···O6 is more symmetric than O5—H5···O2. On the one hand, O1—H1 is remarkably elongated and not only longer than O5—H5 but also than all N—H bonds. On the other hand, O6···H1 represents by far the shortest among all *X*···H interactions in this structure. Although it is tempting to extend this discussion to the comparison of the N—H···N bonds, this is most probably not justified: Allen & Bruno (2010) recently compiled *X*—H bond distances based on neutron diffraction and found shorter average N—H bond lengths in $NH_2$ than in NH groups. In view of these results it is not surprising that interaction C in Fig. 2, the only NH moiety in (1), represents the longest nitrogen–hydrogen bond in this structure.

The second criterion for the strength of hydrogen bonds, electron density, also benefits from the fact that low-temperature neutron diffraction data are available; results from such an experiment allow the description of the anisotropic displacement of H atoms reliably and thus help to deconvolute vibrational and electronic effects on the experimental charge density. Details on the transfer of anisotropic displacement parameters from neutron to X-ray diffraction data are provided in §2. We wish to emphasize that the popular approach for the generation of anisotropic displacement parameters for H atoms (Madsen, 2006) based on extrapolation of rigid-body motions (Schomaker & Trueblood, 1968) cannot be reliably applied for the present study where the most interesting H atoms are involved in short contacts between adjacent residues. Wozniak and coworkers (Hoser *et al.*, 2009) have recently documented the relevance of both precise H-atom positions and H-atom displacement parameters for charge-density studies of hydrogen-bonded systems. High-resolution X-ray diffraction obviously represents the undisposable source of information for an experimental charge-density determination. An atom-centered multipole model was used for the refinement (Volkov *et al.*, 2006), and the resulting electron-density maps have been interpreted according to the Atoms in Molecules approach of Bader (1990). The results confirm that all conventional bonds are associated with bond-critical points (*cf.* Table S2 in the supporting information); for the classical hydrogen bonds (3, −1) critical points are not only detected in the donor–hydrogen but also in the hydrogen···acceptor part of the interactions. The electron density $\rho$ in the bond-critical points of these H···*A* interactions represents an intuitive criterion for characterizing the hydrogen bonds. Table 2 shows that this quantity, $\rho_{bcp}$, amounts to 0.64 (2) e Å$^{-3}$ for the shortest interaction *A* and decreases for longer hydrogen···acceptor distances. The non-classical contact *E*, C9—H9*A*···O6, is associated with an electron density of 0.072 (4) e Å$^{-3}$ in the H···*A* bond-critical point, in good agreement with previous reports for similar interactions (Gatti *et al.*, 2002; Chen *et al.*, 2007; Munshi *et al.*, 2006; Hübschle *et al.*, 2008). Based on theoretical charge densities, Koch & Popelier (1995) have established a set of criteria which allow one to decide whether C—H···O contacts should be addressed as hydrogen bonds; the interaction *E* in Fig. 2 fulfills those among these criteria which can be studied based on experimental data. Espinosa and coworkers have successfully correlated $\rho_{bcp}$ and several

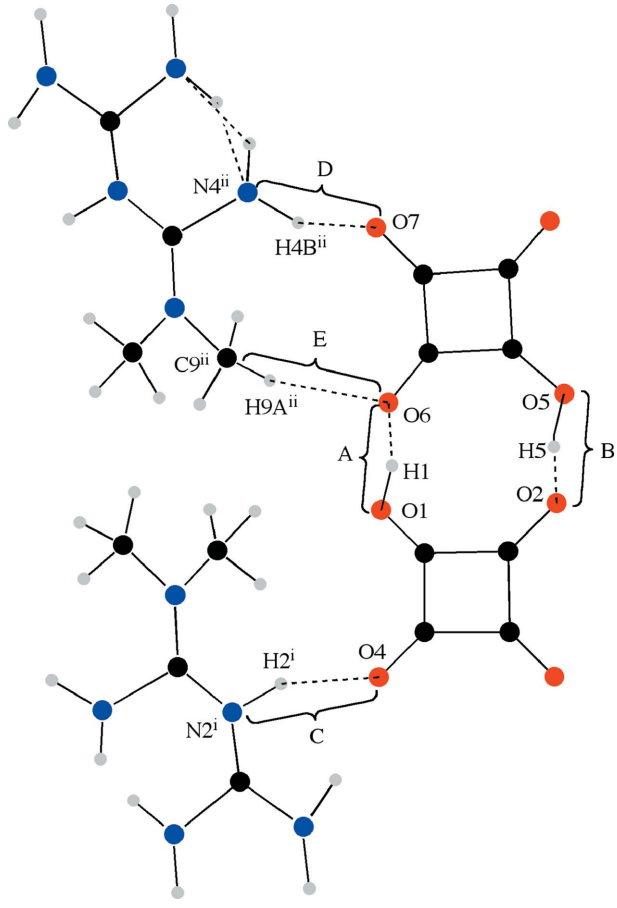


**Figure 2**
Selected hydrogen bonds of different strength in (1). Symmetry codes: (i) $1+x, 1+y, z$; (ii) $2-x, 1-y, 1-z$.

quantities derived from the electron density with H···*A* distances in hydrogen bonds; their correlations hold true over a wide range of hydrogen···acceptor distances (Mata *et al.*, 2010). Our experimental data for the five hydrogen bonds in Table 2 and their good agreement with the linear relationship between ln $\rho_{bcp}$ and the H···*A* distance as identified by Espinosa *et al.* (Mata *et al.*, 2010) are summarized in Fig. 3.

The five hydrogen bonds *A*–*E* described in Table 2 cover the full range from weak and non-classical to very short interactions and hence may be rather different in nature; nevertheless, the associated electron density in the bond-critical point of the H···*A* contact fit the linear relationship rather well. The Laplacian of the electron density represents a more sensitive tool for establishing the closed-shell or shared character of an interaction. With respect to this quantity, our experimental data indicate a clear discrepancy from linear behaviour: As far as the hydrogen bonds *E*–*C* in Fig. 2 with donor···acceptor distances longer than 2.5 Å are concerned, $\nabla^2\rho$ in the bond-critical point assumes small and positive values. This behaviour is in agreement with the correlations established by Espinosa *et al.* for closed-shell interactions and with the classification by Munshi and Row of hydrogen bonds with H···acceptor distances longer than 1.5 Å (Munshi & Row, 2005). However, for the shortest contacts *B* and, in particular, *A*, this trend is significantly inverted: Fig. 4 shows that for the O—H···O interactions smaller positive values of the Laplacian are found than expected from the logarithmic relationship derived by Mata *et al.* (2010).

Our experimental results confirm the tendency observed by Sathyamurthy and co-workers (Parthasarathi *et al.*, 2006) in a theoretical study of hydrogen bonds. When the Laplacian of the electron density is accepted as a criterion for the character of a chemical bond, the shortest hydrogen bond in (1) may be addressed as a shared interaction. Piccoli and coauthors have undertaken a charge density study on tetraacetylethane (Piccoli *et al.*, 2008). At 20 K, the temperature of their X-ray diffraction experiment, the shortest intramolecular hydrogen bond in their system is geometrically rather similar to the shortest O—H···O contact *A* in our title compound. This similarity is not confined to geometry but extends to charge-density features: The electron densities in both bond-critical points of the shorter O—H and the longer H···O interactions are also comparable. The shorter part of the asymmetric hydrogen bond is associated with a strongly negative Laplacian in either case. For the H···O contact in the short hydrogen bond, Piccoli *et al.* report a small negative value, to be compared with +2.43 (5) e Å$^{-5}$ in (1).

An alternative and very sensitive contribution to the classification of the hydrogen bonds in (1) may be from energy-density considerations. The interplay of the (positive) kinetic energy density *G* and the (negative) potential energy density *V* results in negative values $H = G + V$ at the (3, −1) critical point of covalent interactions (Cremer & Kraka, 1984). When the hydrogen bonds compiled in Table 2 are investigated with respect to this criterion, the shortest interaction O1—H1···O6 (*A* in Fig. 2) differs from all the others; it is the only hydrogen bond associated with significantly negative total energy density in the bond-critical point. The same fact can alternatively be perceived in the ratio $|V|/G$: this quantity ranges around unity for the hydrogen bonds *B*–*E* in Fig. 2, indicating a depletion of electrons at the bond-critical points and therefore essentially the closed-shell character of these interactions, whereas hydrogen bond *A* with $|V|/G = 1.66$ can be classified as at least partially covalent (Espinosa *et al.*, 2002). When expressed in atomic units, the ratio $G/\rho_{bcp}$ typically ranges around 1 in closed-shell interactions (Bader, 1990; Macchi & Sironi, 2003), whereas values of *ca* 0.3 are commonly encountered for covalent bonds. Again, the very short hydrogen bond *A* must be considered a special case in between these categories.

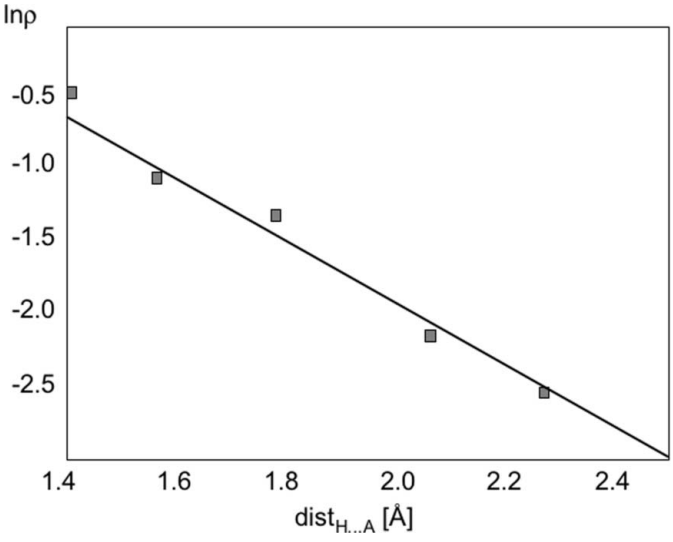


**Figure 3**
Experimental data points ln $\rho_{bcp}$, dist(H···*A*) for the hydrogen bonds in Table 2 and linear relationship ln $\rho_{bcp}$ = 2.4–2.16 × dist(H···*A*) (straight line, *cf.* Mata *et al.*, 2010).

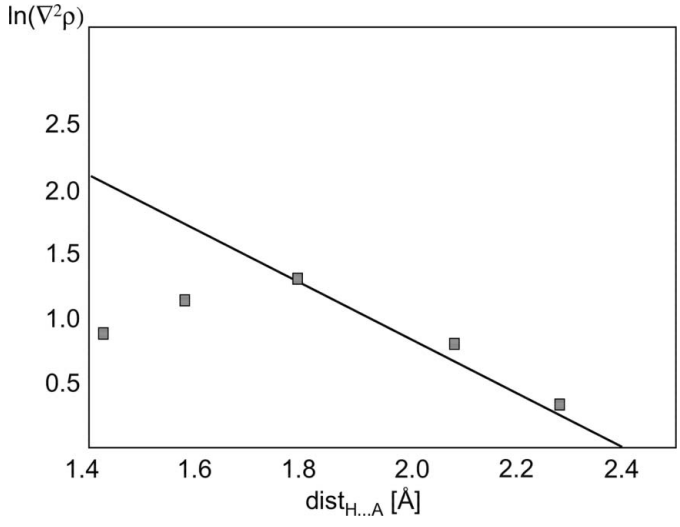


**Figure 4**
Experimental data points ln$\nabla^2\rho_{bcp}$, dist(H···*A*) for the hydrogen bonds in Table 2 and linear relationship ln$\nabla^2\rho_{bcp}$ = 5.1–2.14 × dist(H···*A*) (straight line, *cf.* Mata *et al.*, 2010).

Although the emphasis of this contribution is on the electron density associated with hydrogen bonds, two details concerning the analysis of strong and doubtlessly covalent bonds merit discussion here:

(i) In the dianionic pair in (1), the consequences of the ring strain for chemical bonding in the four-membered hydrogensquarate carbon cycles are reflected in the bond paths and can be perceived in Fig. 5.

The bond-critical points do not coincide with the midpoint of the C—C vectors but are slightly displaced to the periphery, showing a tendency towards 'banana bonds' (Hoffmann & Davidson, 1971; Wiberg, 1996). Consequently, the bond paths for the intra-ring bonds are longer than the corresponding interatomic distances, whereas no significant differences occur for C—N or C—O bonds.

(ii) The distance patterns for hydrogen and strong covalent bonds in (1) are correlated: The exocyclic bonds between C and those O atoms closer to the bridging H atoms, *i.e.* C1—O1 and C5—O5, are not only significantly longer but also associated with a lower electron density than those between carbon and the formally anionic oxygen atoms, C2—O2 and C6—O6.

A list compiling features of the electron density in the bond-critical points for all strong covalent bonds in the title compound is supplied in Table S2 of the supporting information.

## 4. Conclusions

The title compound enabled us to directly compare very different hydrogen bonds with respect to sensitive criteria. One of its hydrogen bonds is characterized by a very short donor···acceptor distance. The result of the single-crystal neutron diffraction experiment allowed us to classify this shortest hydrogen bond as more symmetric than usual, with a significantly elongated donor–hydrogen bond and a rather short hydrogen···acceptor contact. Direct comparison has been made to strong and moderately strong classical and to weak non-classical $X$—H···O interactions in the same crystal structure. The primary result of the high-resolution X-ray diffraction study, *i.e.* the electron density in the bond-critical point of the H···O contacts, follows the simple relationship recently suggested by Espinosa and co-workers (Mata *et al.*, 2010); therefore, this property alone does not qualify the shortest O—H···O bond as unique. However, the more sensitive criteria such as the Laplacian, the total energy density and the ratio $G/\rho_{bcp}$ reveal that the shortest hydrogen bond in (1) does not simply follow the trend of the longer contacts but rather represents a borderline case in-between a covalent and a closed-shell interaction. Charge-density studies of hydrogen bonds based on multipole refinements (Espinosa *et al.*, 1998) or, alternatively, on the Maximum Entropy Method (Netzel & van Smaalen, 2009) for the treatment of diffraction data agree about exponential relationships between the H···O distance and properties in the bond-critical point but

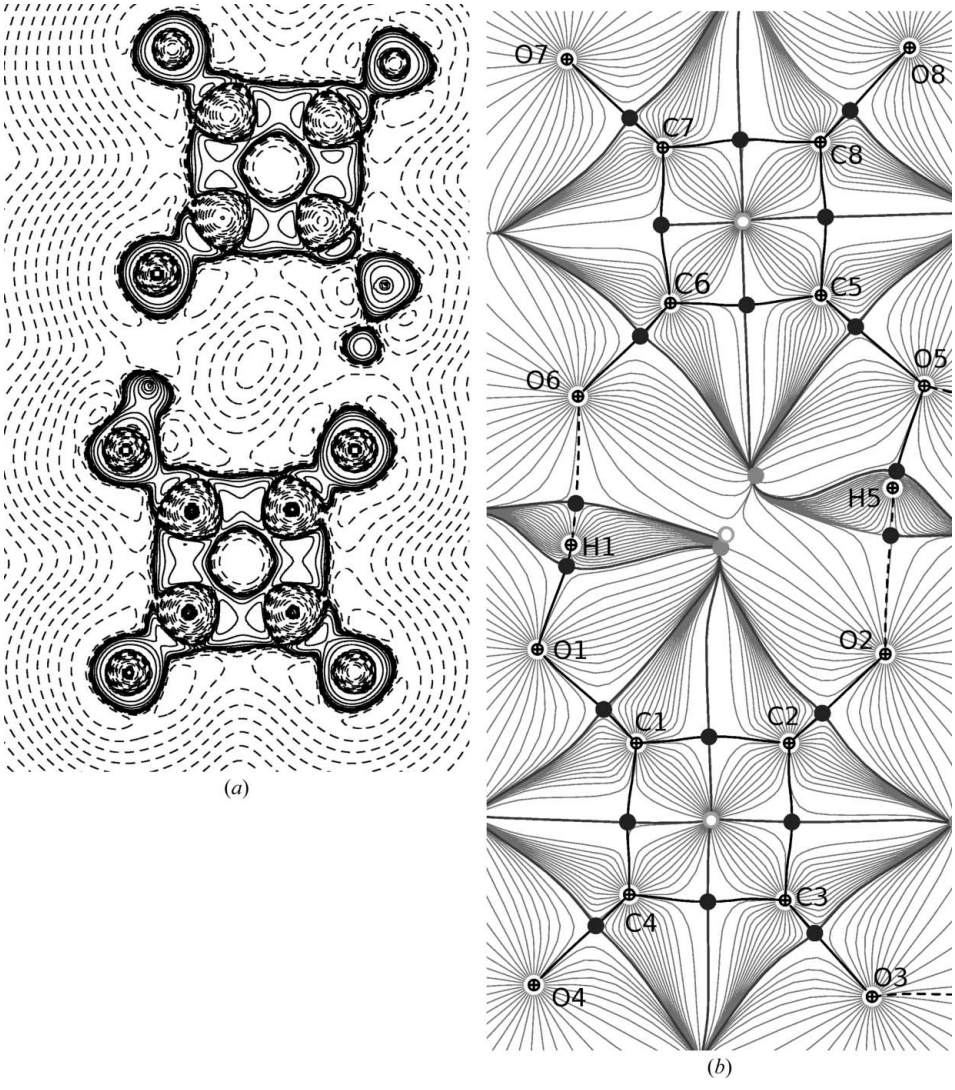


**Figure 5**
(*a*) Laplacian of the electron density at [$\pm 2^n \times 10^{-3}$ e Å$^{-5}$ ($0 \leq n \leq 20$), negative values solid] and (*b*) gradient trajectories, (3, −1) critical points (black), (3, +1) critical points (white) and (3, +3) critical points (grey) in the dianion in (1).

deduce different limits for covalency, expressed in the ratio $|V|/G$: According to the relationship established by Espinosa *et al.* (1998), this limit is encountered at a H···O distance of 1.33, whereas Netzel and van Smaalen expect it at 1.47 Å. For the shortest hydrogen bond in (1), geometric and electronic criteria consistently indicate a significant degree of covalency; the interaction is characterized by a H···O distance of 1.421 (4) Å and a $|V|/G$ ratio of 1.66, and hence falls in the region between the lower and upper limit. Their discrepancy should not be overestimated: longer hydrogen bonds dominate both compilations, and extrapolation is required. Standard uncertainties in charge-density studies are often underestimated, and when average values for chemical bonding in different systems are taken into consideration, smooth transitions rather than clearcut limits should be expected.

This work was supported by DFG, priority program 1178, Experimental Charge Density as the Key to Understand Chemical Interactions. MDS is grateful to DAAD for financial support.

## References


Allen, F. H. & Bruno, I. J. (2010). *Acta Cryst.* B**66**, 380–386.
Bader, R. F. W. (1990). *Atoms in Molecules: A Quantum Theory*. Oxford: Clarendon Press.
Braga, D., Maini, L., Polito, M., Tagliavini, E. & Grepioni, F. (2003). *Coord. Chem. Rev.* **246**, 53–71.
Bruker (2003). *SAINT+*, Version 6.45. Bruker AXS Inc., Madison, Wisconsin, USA.
Chen, Y.-S., Stash, A. I. & Pinkerton, A. A. (2007). *Acta Cryst.* B**63**, 309–318.
Cordero, B., Gómez, V., Platero-Prats, A. E., Revés, M., Echeverría, J., Cremades, E., Barragán, F. & Alvarez, S. (2008). *Dalton Trans.* pp. 2832–2838.
Cremer, D. & Kraka, E. (1984). *Angew. Chem. Int. Ed. Engl.* **23**, 627–628.
Desiraju, G. R. (1995). *Angew. Chem.* **107**, 2541–2558.
Espinosa, E., Alkorta, I., Elguero, J. & Molins, E. (2002). *J. Chem. Phys.* **117**, 5529–5542.
Espinosa, E., Molins, E. & Lecomte, C. (1998). *Chem. Phys. Lett.* **285**, 170–173.
Flensburg, C., Larsen, S. & Stewart, R. F. (1995). *J. Phys. Chem.* **99**, 10130–10141.
Gatti, C., May, E., Destro, R. & Cargnoni, F. (2002). *J. Phys. Chem. A*, **106**, 2707–2720.
Gilli, P., Bertolasi, V., Ferretti, V. & Gilli, G. (1994). *J. Am. Chem. Soc.* **116**, 909–915.
Gilli, P., Bertolasi, V., Pretto, L., Ferretti, V. & Gilli, G. (2004). *J. Am. Chem. Soc.* **126**, 3845–3855.
Gilli, P., Pretto, L., Bertolasi, V. & Gilli, G. (2009). *Acc. Chem. Res.* **42**, 33–44.
Hansen, N. K. & Coppens, P. (1978). *Acta Cryst.* A**34**, 909–921.
Hirshfeld, F. L. (1976). *Acta Cryst.* A**32**, 239–244.
Hoffmann, R. & Davidson, R. (1971). *J. Am. Chem. Soc.* **93**, 5699–5705.
Hoser, A. A., Dominiak, P. M. & Woźniak, K. (2009). *Acta Cryst.* A**65**, 300–311.
Hu, C. & Englert, U. (2005). *Angew. Chem. Int. Ed.* **44**, 2281–2283.
Hu, C., Huster, J. & Englert, U. (2003). *Z. Kristallogr.* **218**, 761–765.
Hübschle, C. B., Dittrich, B., Grabowsky, S., Messerschmidt, M. & Luger, P. (2008). *Acta Cryst.* B**64**, 363–374.
Kaljurand, I., Rodima, T., Leito, I., Koppel, I. A. & Schwesinger, R. (2000). *J. Org. Chem.* **65**, 6202–6208.
Karle, I. L., Ranganathan, D. & Haridas, V. (1996). *J. Am. Chem. Soc.* **118**, 7128–7133.
Koch, U. & Popelier, P. L. A. (1995). *J. Phys. Chem.* **99**, 9747–9754.
Kostansek, E. C. & Busing, W. R. (1972). *Acta Cryst.* B**28**, 2454–2459.
Lamberts, K., Kalf, I., Ramadan, A., Müller, P., Dronskowski, R. & Englert, U. (2011). *Polymers*, **3**, 1151–1161.
LeBel, O., Maris, T., Duval, H. & Wuest, J. D. (2005). *Can. J. Chem.* **83**, 615–625.
Limbach, H.-H. & Manz, J. (1998). *Ber. Bunsenges. Phys. Chem.* **102**, 289–586.
Macchi, P. & Sironi, A. (2003). *Coord. Chem. Rev.* **238–239**, 383–412.
Madsen, A. Ø. (2006). *J. Appl. Cryst.* **39**, 757–758.
Mata, I., Alkorta, I., Molins, E. & Espinosa, E. (2010). *Chem. Eur. J.* **16**, 2442–2452.
Munshi, P. & Row, T. N. G. (2005). *CrystEngComm*, **7**, 608–611.
Munshi, P., Thakur, T. S., Row, T. N. G. & Desiraju, G. R. (2006). *Acta Cryst.* B**62**, 118–127.
Netzel, J. & van Smaalen, S. (2009). *Acta Cryst.* B**65**, 624–638.
Neumann, M., Brogham, D. F., McGloin, C. J., Johnson, M. R., Horsewill, A. J. & Tromsdorff, H. P. (1998). *J. Chem. Phys.* **109**, 7300–7311.
Nowick, J. S. (2008). *Acc. Chem. Res.* **41**, 1319–1330.
Parthasarathi, R., Subramanian, V. & Sathyamurthy, N. (2006). *J. Phys. Chem. A*, **110**, 3349–3351.
Piccoli, P. M., Koetzle, T. F., Schultz, A. J., Zhurova, E. A., Stare, J., Pinkerton, A. A., Eckert, J. & Hadzi, D. (2008). *J. Phys. Chem. A*, **112**, 6667–6677.
Prins, L. J., Reinhoudt, D. N. & Timmerman, P. (2001). *Angew. Chem. Int. Ed.* **40**, 2382–2426.
Rodrigues, B. L., Tellgren, R. & Fernandes, N. G. (2001). *Acta Cryst.* B**57**, 353–358.
Roesky, H. W. & Andruh, M. (2003). *Coord. Chem. Rev.* **236**, 91–119.
Schomaker, V. & Trueblood, K. N. (1968). *Acta Cryst.* B**24**, 63–76.
Şerb, M.-D. (2009). Doctoral dissertation, University Politehnica of Bucharest and RWTH Aachen University.
Sheldrick, G. M. (2008). *Acta Cryst.* A**64**, 112–122.
Spek, A. L. (2009). *Acta Cryst.* D**65**, 148–155.
Steiner, T. (2002). *Angew. Chem. Int. Ed.* **41**, 48–76.
Sutcliffe, M. J. & Scrutton, N. S. (2002). *Eur. J. Biochem.* **269**, 3096–3102.
Volkov, A., Macchi, P., Farrugia, L. J., Gatti, C., Mallinson, P. R., Richter, T. & Koritsanszky, T. (2006). *XD*2006. University of New York at Buffalo, USA.
Wiberg, K. B. (1996). *Acc. Chem. Res.* **29**, 229–234.
Wilson, C. C. (2001). *Acta Cryst.* B**57**, 435–439.